Dynamical Behavior and Exact Traveling Wave Solutions for Three Special Variants of the Generalized Tzitzeica Equation*

Rongzheng Shu[1], Haohao Qian[1] and Lina Zhang[1,†]

Abstract The dynamics and bifurcations of traveling wave solutions are studied for three nonlinear wave equations. A new phenomenon, such as a composed orbit, which consists of two or three heteroclinic orbits, may correspond to a solitary wave solution, a periodic wave solution or a peakon solution, is found for the equations. Some previous results are extended.

Keywords Generalized Tzitzeica equation, Solitary wave solution, Periodic wave solution, Peakon solution.

MSC(2010) 34C23, 37G10, 37G15.

1. Introduction

The generalized Tzitzeica equation

$$u_{xt} = ae^{mu} + be^{nu}, \tag{1.1}$$

where a, b are arbitrary constants and m, n are integers. Specially, when $m = 1$ and $n = -2$, equation (1.1) is called the Tzitzeicta equation, which was originally found from the work of Tzitzeica [14]. Later on, Dodd, Bullough and Mikhailov [4, 12] introduced some other forms of the evolution equation involving the exponential term e^{pu}. For $m = 1$ and $n = -1$, equation (1.1) reduces to the sinh-Gordon equation. For $m = 1$ and $n = -2$, equation (1.1) turns into the Dodd–Bullough–Mikhailov equation. For $m = -1$ and $n = -2$, equation (1.1) gives rise to the Tzitzeica–Dodd–Bullough equation. These well-known equations have extensive applications in mathematical biology, nonlinear optics, fluid mechanics, chemical kinetics and quantum field theory [7, 13, 18]. Particularly in recent years, many researchers have focused on the search for exact solutions of nonlinear wave equations by using different methods and techniques. Among others, Wazwaz [15] derived some traveling wave solutions for the above three variants of the generalized Tzitzeica equation (1.1) by employing the tanh method and extended tanh method.

Abazari [1] applied the (G'/G)-method for constructing solitons and periodic solutions for the generalized Tzitzeica equation (1.1). In fact, it is important to understand the dynamical behavior of traveling wave solutions for nonlinear wave equations [3, 5, 6, 8–11, 16, 17, 19–22]. In [5], Chen et al., studied the qualitative behavior of the traveling wave solutions of the generalized Tzitzeica equation (1.1) in the case of degenerate equilibrium points.

In this paper, we carry out further study on the dynamical behavior and exact traveling wave solutions of the three variants of equation (1.1). By presenting some representative bifurcation diagrams under different parametric conditions, not only some new exact explicit expressions of traveling wave solutions including solitary wave solutions, periodic wave solutions and peakon solutions are obtained, but also some interesting phenomena arise. For instance, a composed orbit, which consists of two or three heteroclinic orbits, may correspond to a solitary wave solution, a periodic wave solution or a peakon solution. This work complements the previous results of [5].

2. Phase portraits of three variants of the generalized Tzitzeica equation

To study the equilibrium points and their properties of the corresponding traveling wave system of the generalized Tzitzeica equation, we need to introduce some preliminaries [2] first.

Lemma 1. Suppose $p \in R$ be an equilibrium point of the planar polynomial integrable system

$$\dot{x} = P(x,y), \quad \dot{y} = Q(x,y). \tag{2.1}$$

Denote $\Delta = P_x(p)Q_y(p) - P_y(p)Q_x(p)$ and $T = P_x(p) + Q_y(p)$. If $\Delta < 0$, then p is a saddle point. If $T^2 > 4\Delta > 0$, then p is a node (stable if $T < 0$, unstable if $T > 0$). If $T = 0 < \Delta$, then p is a center. Moreover, if $\Delta = T = 0$ and the Jacobian matrix at the point p is not the zero matrix, then p is a nilpotent point.

2.1. Phase portraits of the sinh-Gordon equation

For $m = 1$ and $n = -1$, equation (1.1) reduces to the sinh-Gordon equation

$$u_{xt} = ae^u + be^{-u}. \tag{2.2}$$

We look for the traveling wave solutions of equation (2.2) in the form of $u(x,t) = u(\xi)$ with $\xi = x - ct$. Inserting it into equation (2.2) and subsequently making the variable transformation $v = e^u$, we have

$$cvv'' - c(v')^2 + av^3 + bv = 0. \tag{2.3}$$

Letting $y = v'$ in equation (2.3) generates a planar system

$$\frac{dv}{d\xi} = y, \quad \frac{dy}{d\xi} = \frac{cy^2 - av^3 - bv}{cv} \tag{2.4}$$

with the first integral

$$H(v,y) = \frac{cy^2 + 2av^3 - 2bv}{cv^2} = h. \tag{2.5}$$

System (2.4) is a singular traveling wave system, because the second equation of (2.4) is discontinuous on the straight line $v = 0$. Making the transformation $\mathrm{d}\xi = cv\,\mathrm{d}\tau$ carries (2.4) into the associated regular system

$$\frac{\mathrm{d}v}{\mathrm{d}\tau} = cvy, \quad \frac{\mathrm{d}y}{\mathrm{d}\tau} = cy^2 - av^3 - bv. \tag{2.6}$$

System (2.6) has the same first integral as system (2.4). However, systems (2.4) and (2.6) define different vector fields on the two sides of the straight line $v = 0$.

Obviously, for $ab > 0$, system (2.6) has only one equilibrium point $O(0,0)$ on the v-axis. Upon further analysis, it can be concluded that $O(0,0)$ is a nilpotent elliptic-saddle point with one separatrix is tangent to the semi-axis $y > 0$, and the other to the semi-axis $y < 0$.

For $ab < 0$, system (2.6) has three equilibrium points $O(0,0)$ and $E_{1,2}(v_{1,2},0)$ on the v-axis, where $v_1 = \sqrt{-\frac{b}{a}}$ and $v_2 = -\sqrt{-\frac{b}{a}}$. After analysis, we know that the equilibrium point $O(0,0)$ remains to be a nilpotent elliptic-saddle point. In the meantime, corresponding to the equilibrium points $E_{1,2}(v_{1,2},0)$, $\Delta = -2bcv_{1,2}$ and $T = 0$. Hence, we arrive that $E_1(v_1,0)$ is a saddle point, while $E_2(v_2,0)$ is a center, if $bc > 0$ or $E_1(v_1,0)$ a center, while $E_2(v_2,0)$ a saddle point, if $bc < 0$.

Based on the above discussion and without loss of generality, we draw the phase portraits of system (2.4) for $b > 0$ and $c > 0$ in the (v,y)-phase plane, which are shown in Figure 1.

(a) $a < 0$ (b) $a > 0$
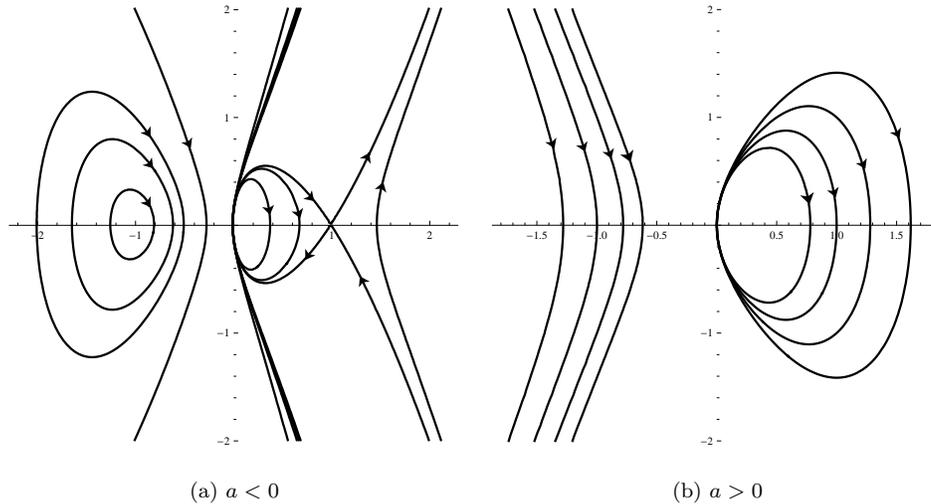
Figure 1. The vector fields and phase portraits of system (2.4), when $b > 0$ and $c > 0$

2.2. Phase portraits of the Dodd–Bullough–Mikhailov equation

For $m = 1$ and $n = -2$, equation (1.1) becomes the Dodd–Bullough–Mikhailov equation

$$u_{xt} = ae^u + be^{-2u}. \tag{2.7}$$

Letting $u(x,t) = u(\xi)$, $\xi = x - ct$ and using the Painlevé property $v = e^u$ convert equation (2.7) into the traveling wave system

$$\frac{\mathrm{d}v}{\mathrm{d}\xi} = y, \quad \frac{\mathrm{d}y}{\mathrm{d}\xi} = \frac{cy^2 - av^3 - b}{cv}, \tag{2.8}$$

which has the first integral

$$H(v,y) = \frac{cy^2 + 2av^3 - b}{cv^2} = h. \tag{2.9}$$

Letting $\mathrm{d}\xi = cv\,\mathrm{d}\tau$, system (2.8) becomes the following regular system

$$\frac{\mathrm{d}v}{\mathrm{d}\tau} = cvy, \quad \frac{\mathrm{d}y}{\mathrm{d}\tau} = cy^2 - av^3 - bv. \tag{2.10}$$

Systems (2.8) and (2.10) have the same topological phase portraits since both of them have the same first integral (2.9). However, the fact that systems (2.8) and (2.10) define different vector fields on the two sides of the straight line $v = 0$ indicates that the dynamical behavior of the orbits of system (2.8) in the neighborhood of the straight line $v = 0$ needs to be handled delicately.

It is easy to check that system (2.10) has a unique equilibrium point $E_1(v_1, 0)$ on the v-axis, where $v_1 = \sqrt[3]{-\frac{b}{a}}$. When $bc > 0$, in addition to the equilibrium point $E_1(v_1, 0)$, system (2.10) has a pair of equilibrium points $S_\pm(0, \pm Y_s)$ on the straight line $v = 0$, where $Y_s = \sqrt{\frac{b}{c}}$. Corresponding to the equilibrium point $E_1(v_1, 0)$, $\Delta = -3bc$ and $T = 0$. Therefore, $E_1(v_1, 0)$ is a saddle point if $bc > 0$, a center if $bc < 0$. As to the equilibrium points $S_\pm(0, \pm Y_s)$, we have $\Delta = 2bc$, $T = \pm 3\sqrt{bc}$ and $T^2 > 4D > 0$. Hence, $S_+(0, Y_s)$ is an unstable node, while $S_-(0, -Y_s)$ is a stable node.

On the basis of above qualitative analysis and for the sake of brevity, under two different parameter conditions, we have the bifurcations of phase portraits of system (2.8) shown in Figure 2.

(a) $c > 0$ (b) $c < 0$
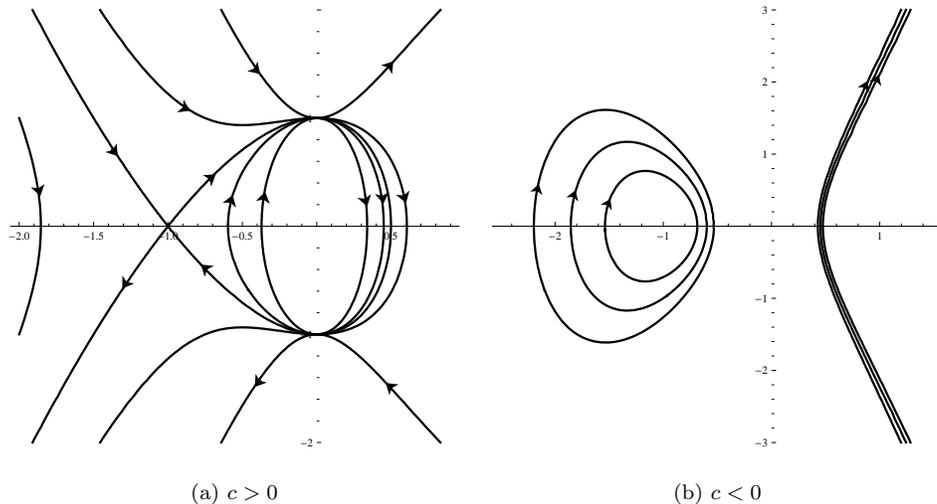
Figure 2. The vector fields and phase portraits of system (2.8), when $a > 0$ and $b > 0$

2.3. Phase portraits of the Tzitzeica–Dodd–Bullough equation

For $m = -1, n = -2$, equation (1.1) reduces to the Tzitzeica–Dodd–Bullough equation

$$u_{xt} = ae^{-u} + be^{-2u}. \tag{2.11}$$

Equation (2.11) can be cast into the following planar system

$$\frac{\mathrm{d}v}{\mathrm{d}\xi} = y, \quad \frac{\mathrm{d}y}{\mathrm{d}\xi} = \frac{cy^2 - av - b}{cv} \tag{2.12}$$

with the first integral

$$H(v, y) = \frac{cy^2 - 2av - b}{cv^2} = h, \tag{2.13}$$

where $u(x, t) = u(x - ct)$, $\xi = x = ct$ and $v = e^u$. Letting $\mathrm{d}\xi = cv\,\mathrm{d}\tau$ carries (2.12) into the associated regular system

$$\frac{\mathrm{d}v}{\mathrm{d}\tau} = cvy, \quad \frac{\mathrm{d}y}{\mathrm{d}\tau} = cy^2 - av - b, \tag{2.14}$$

which has the same first integral as system (2.12).

In order to make clear the dynamical behavior of orbits in the vicinity of the straight line $v = 0$ of system (2.12), first of all, we need to study the equilibrium points and their properties of system (2.14). Apparently, system (2.14) has a unique equilibrium point $E_1(v_1, 0)$ on the v-axis, where $v_1 = -\frac{b}{a}$. When $bc > 0$, system (2.10) has a pair of equilibrium points $S_\pm(0, \pm Y_s)$ on the straight line $v = 0$, where $Y_s = \sqrt{\frac{b}{c}}$. Moreover, with the help of Lemma 1, we know that $E_1(v_1, 0)$ is a saddle point if $bc > 0$, a center if $bc < 0$, and $S_\pm(0, \pm Y_s)$ are two nodes. Under two different parameter conditions, we have the bifurcations of phase portraits of system (2.12), which are shown in Figure 3.

(a) $c > 0$ (b) $c < 0$
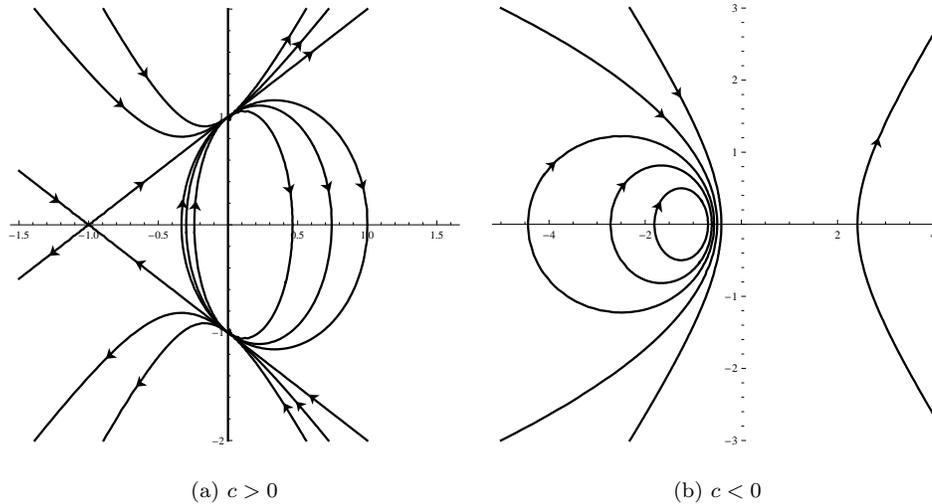
Figure 3. The vector fields and phase portraits of system (2.12), when $a > 0$ and $b > 0$

3. Main results and the theoretic derivations of main results

In this section, we summarize the main results in the following theorems, which will be followed by the proofs.

Theorem 1. For $a < 0$, $b > 0$ and $c > 0$, equation (2.2) has one solitary wave solution

$$v(x,t) = \sqrt{-\frac{b}{a}} \tanh^2\left(\sqrt{-\frac{ab}{4c^2}}(x - ct)\right). \tag{3.1}$$

Two families of periodic wave solutions

$$v(x,t) = r_{12}\,\mathrm{sn}^2\left(\sqrt{-\frac{ar_{11}}{2c}}(x - ct), k_1\right), \tag{3.2}$$

$$v(x,t) = r_{22} + (r_{21} - r_{22})\,\mathrm{sn}^2\left(\sqrt{\frac{ar_{22}}{2c}}(x - ct), k_2\right), \tag{3.3}$$

where $k_1 = \sqrt{\frac{r_{12}}{r_{11}}}$ and $k_2 = \sqrt{\frac{r_{22}-r_{21}}{r_{22}}}$ with $r_{22} < r_{21} < 0 < r_{12} < r_{11}$.

Proof. Let $h_i = H(v_i, 0)$, $i = 1, 2$, where $H(v, y)$ is given in (2.5). Then, corresponding to the level set defined by $H(v, y) = h_1$ in Figure 1(a), there exist two curves which are tangent to the straight line $v = 0$ at the elliptic-saddle point $O(0, 0)$ and intersect with the v-axis at the saddle point $E_1(v_1, 0)$. These two curves can be seen as a compounded homoclinic orbit of system (2.4) to the saddle point $E_1(v_1, 0)$, which can be expressed as

$$y = \sqrt{\frac{2v}{c}}(\sqrt{-av} - \sqrt{b})\,\mathrm{sgn}(\xi), \quad v \in [0, v_1). \tag{3.4}$$

Integrating the first equation of (2.4) along the combined homoclinic orbit (3.4) leads to the explicit representation of the solitary wave solution (3.1).

In addition, corresponding to the level sets defined by $H(v, y) = h, h \in (-\infty, h_1)$ in Figure 1(a), there exist a family of closed orbits which are tangent to the straight line $v = 0$ at the elliptic-saddle point $O(0, 0)$ and are enveloped in the combined homoclinic orbit. These closed orbits can be seen as combined periodic orbits of system (2.4), which can be expressed as

$$y^2 = \frac{2a}{c}v(r_{11} - v)(v - r_{12}), \quad v \in [0, r_{12}], \tag{3.5}$$

where $r_{11} = \frac{ch+\sqrt{c^2h^2+16ab}}{4a}$ and $r_{12} = \frac{ch-\sqrt{c^2h^2+16ab}}{4a}$. With the aid of equation (3.5) and $\frac{dv}{d\xi} = y$, we infinitely obtain many elliptic functions of periodic wave solutions (3.2).

Similarly, corresponding to the periodic orbits surrounding the center $E_2(v_2, 0)$, defined by $H(v, y) = h, h \in (h_2, +\infty)$ in Figure 1(a), we get the parametric representations of periodic wave solutions (3.3). $\square$

Remark 1. The solitary wave solution (3.1) corresponds to a composed homoclinic orbit, which is composed of two heteroclinic orbits of system (2.6). Besides, the

dynamical behaviors of the periodic wave solutions of (3.2) and (3.3) are completely different in spite of similar analytical expressions. The periodic wave solutions (3.2) correspond to a family of composed periodic orbits, which constitute a family of homoclinic orbits of system (2.6), while the periodic wave solutions (3.3) correspond to a family of periodic orbits of system (2.4).

Theorem 2. For $a > 0$, $b > 0$ and $c > 0$, equation (2.7) has one solitary wave solution

$$v(x,t) = \frac{3v_1 \tanh^2\left(\sqrt{\frac{-3av_1}{4c}}(x-ct)\right) - v_1}{2}. \tag{3.6}$$

One family of periodic wave solutions

$$v(x,t) = \frac{(r_{31} - r_{33})r_{32} - (r_{31} - r_{32})\operatorname{sn}^2\left(\sqrt{\frac{a(r_{31}-r_{33})}{2c}}(x-ct), k_3\right)}{(r_{31} - r_{33}) - (r_{31} - r_{32})\operatorname{sn}^2\left(\sqrt{\frac{a(r_{31}-r_{33})}{2c}}(x-ct), k_3\right)}, \tag{3.7}$$

where $k_3 = \sqrt{\frac{r_{31}-r_{32}}{r_{32}-r_{33}}}$ with $r_{33} < r_{32} < 0 < r_{31}$.

Proof. Let $h_1 = H(v_1, 0) = -\frac{3}{c}\sqrt[3]{a^2 b}$, where $H(v, y)$ is given in (2.9). Then, corresponding to the level set defined by $H(v, y) = h_1$ in Figure 2(a), there exist three curves which connect the saddle point $E_1(v_1, 0)$ and the two nodes $S_{\pm}(0, \pm Y_s)$ respectively. These three curves can be seen as a composed homoclinic orbit of system (2.12) to the saddle point $E_1(v_1, 0)$, which can be written as

$$y = -\sqrt{\frac{a}{c}}(v - v_1)\sqrt{-2v - v_1}\operatorname{sgn}(\xi), \quad v \in (v_1, -\frac{v_1}{2}]. \tag{3.8}$$

Integrating the first equation of (2.12) along the composed homoclinic orbit, (3.8) follows the parametric representation of the solitary wave solution (3.6).

Additionally, for any $h \in (-\infty, h_1)$, the level set defined by $H(v, y) = h$ corresponds to two curves, which connect the two nodes $S(0, \pm Y_s)$ on the right and left sides of the straight line $v = 0$, and are embraced in the composed homoclinic orbits (see Figure 2(a)). These two curves can be regarded as a combined periodic orbit of system (2.12), which can be written as

$$y^2 = \frac{2a}{c}v(r_{31} - v)(v - r_{32})(v - r_{33}), \quad v \in [r_{32}, r_{31}], \tag{3.9}$$

where r_{31}, r_{32}, r_{33} ($r_{33} < r_{32} < 0 < r_{31}$) are three real roots of the algebraic equation $b + chv^2 - 2av^3 = 0$. The combined periodic orbits (3.9) bring about the periodic wave solutions (3.7). $\square$

Remark 2. The solitary wave solution (3.6) corresponds to a composed homoclinic orbit, which consists of three heteroclinic orbits of system (2.10). The periodic wave solutions (3.7) correspond to a family of composed periodic orbits, which constitute two families of heteroclinic orbits of system (2.10).

Theorem 3. For $a > 0$, $b > 0$ and $c > 0$, equation (2.11) has one peakon solution

$$v(x,t) = \frac{1}{a}\exp\left(-\frac{a}{\sqrt{bc}}|x-ct|\right) + c. \tag{3.10}$$

One family of periodic wave solutions

$$v(x,t) = \frac{r_{41} + r_{42}}{2} - \frac{r_{41} - r_{42}}{2} \cos\left(\sqrt{-h}x\right), \tag{3.11}$$

where $r_{42} < 0 < r_{41}$ and $h < 0$.

Proof. The triangular curves, which connect the saddle point $E_1(v_1, 0)$ and the two nodes $S_\pm(0, \pm Y_s)$ respectively, have the level set $H(v, y) = H(v_1, 0) = -\frac{a^2}{bc}$ in Figure 3(a), and can be regarded as a singular homoclinic orbit of system (2.12) to the saddle point $E_1(v_1, 0)$, which can be written as $y^2 = -\frac{1}{bc}(av + b)^2$. By using the first equation of (2.12) to carry out integration along the singular homoclinic orbit, we obtain the peakon solution (3.10).

Additionally, the computation of the periodic wave solution (3.11) is similar to that of (3.7), we omit it for brevity. □

Remark 3. The peakon solution (3.10) corresponds to a singular homoclinic orbit, which comprises three heteroclinic orbits of system (2.14). The periodic wave solutions (3.11) correspond to a family of composed periodic orbits, which comprise two families of heteroclinic orbits of system (2.14).

4. Conclusions

In this work, we provide some new types of solitary wave solutions and periodic wave solutions, which are expressed in terms of hyperbolic and Jacobi elliptic functions (see Theorems 1–3) for three variants of the generalized Tzitzeica equation. In particular, dynamical analysis shows that a composed orbit, which is comprised of two or three heteroclinic orbits, can correspond to a solitary wave solution or a periodic wave solution, and a homoclinic orbit can also correspond to a periodic wave solution. Similar results can also be found in [9, 16, 17].

On the other hand, we have to admit that we discuss only three special cases of the generalized Tzitzeica equation, and we have not consider the general m and n in the current paper yet. Actually, we are applying the approach proposed in this paper to the generalized Tzitzeica equation with general m and n, and have already gotten some new solutions and the abundant dynamical behaviors in them, which we will report in another paper.

References

[1] R. Abazari, *The (G'/G)-expansion method for Tzitzeica type nonlinear evolution equations*, Mathematical and Computer Modelling, 2010, 52(9–10), 1834–1845

[2] A. A. Andronov, et al., *Qualitative Theory of Second-Order Dynamical Systems*, Wiley, New York, 1973.

[3] G. Betchewe, K. K. Victor, B. B. Thomas and K. T. Crepin, *New solutions of the Gardner equation: Analytical and numerical analysis of its dynamical understanding*, Applied Mathematics and Computation, 2013, 223(15), 377–388.

[4] R. K. Bullough and R. K. Dodd, *Polynomial Conserved Densities for the Sine-Gordon Equations*, Proceedings of the Royal Society A, 1977, 352(1671), 481–503.

[5] A. Chen, W. Huang and J. Li, *Qualitative behavior and exact traveling wave solutions of the Zhiber–Shabat equation*, Journal of Computational and Applied Mathematics, 2009, 230(2), 559–569.

[6] A. Chen, S. Wen, S. Tang, W. Huang and Z. Qiao, *Effects of quadratic singular curves in integrable equations*, Studies in Applied Mathematics, 2015, 134(1), 24–61.

[7] E. Infeld and G. Rowlands, *Nonlinear Waves, Solitons and Chaos*, Cambridge University Press, Cambridge, 2000.

[8] T. D. Leta and J. Li, *Various exact soliton solutions and bifurcations of a generalized Dullin–Gottwald–Holm equation with a power law nonlinearity*, International Journal of Bifurcation and Chaos, 2017, 27(8), Article ID 1750129, 22 pages.

[9] J. Li, *Singular Nonlinear Travelling Wave Equations: Bifurcations and Exact Solutions*, Science Press, Beijing, 2013.

[10] J. Li, G. Chen and J. Song, *Exact traveling wave solutions and bifurcations of classical and modified Serre shallow water wave equations*, International Journal of Bifurcation and Chaos, 2019, 29(12), Article ID 1950153, 25 pages.

[11] Q. Meng and B. He, *Dynamical behaviors and exact traveling wave solutions for a modified Broer–Kaup system*, Results in Physics, 2017, 7, 1563–1581.

[12] A. Mikhailov, *The reduction problem and the inverse scattering method*, Physica D, 1981, 3(1–2), 73–117.

[13] A. D. Polyanin and V. F. Zaitsev, *Handbook Of Nonlinear Partial Differential Equations*, Chapman & Hall/CRC, Boca Raton, 2004.

[14] G. Tzitzeica, *Sur une nouvelle classe de surfaces*, Comptes Rendus de l'Academie des Sciences, 1910, 150, 955–956.

[15] A. M. Wazwaz, *The tanh method for traveling wave solutions to the Zhiber–Shabat equation and other related equations*, Communications in Nonlinear Science and Numerical Simulation, 2008, 13(3), 584–592.

[16] Z. Wen, *Bifurcations and exact traveling wave solutions of the celebrated Green–Naghdi equations*, International Journal of Bifurcation and Chaos, 2017, 27(7), Article ID 1750114, 7 pages.

[17] Z. Wen, *Abundant Dynamical Behaviors of Bounded Traveling Wave Solutions to Generalized θ-Equation*, Computational Mathematics and Mathematical Physics, 2019, 59, 926–935.

[18] G. B. Whitham, *Linear and Nonlinear Waves*, Wiley, New York, 1999.

[19] Y. Xu and L. Zhang, *Bifurcations of traveling wave solutions for the nonlinear Schrödinger equation with fourth-order dispersion and cubic-quintic nonlinearity*, Journal of Applied Analysis and Computation, 2020, 10(6), 2722–2733.

[20] L. Zhang, *Nilpotent singular points and smooth periodic wave solutions*, Proceedings of the Romanian Academy Series A, 2019, 20(1), 3–9.

[21] L. Zhang and W. Huang, *Breaking wave solutions of a short wave model, Results in Physics*, 2019, 15, Article ID 102733, 6 pages.

[22] L. Zhang and T. Song, *Traveling wave solutions of a generalized Camassa–Holm equation: a dynamical system approach*, Mathematical Problems in Engineering, 2015, Article ID 610979, 19 pages.